

Microfluidic System for the Study of Cancer Invasion and Intravasation

by
Yu Xu

A thesis submitted to Johns Hopkins University in conformity with the requirements for
the degree of Master of Science and Engineering

Baltimore, Maryland
June 2017

Abstract

Cancer cells in solid tumors often experience low oxygen and nutrition concentrations due to underdeveloped vasculature. Many studies have indicated that the altered oxygen and nutrition levels have profound effects on cancer metastasis, although the exact mechanism is still elusive. Improved understanding of the specific roles of oxygen and nutrition levels on metastasis could lead to the discovery of new therapeutic targets and better treatment methods.

In this project, we aim to develop a microfluidic system to simulate the tumor microenvironment and tumor-vascular interface. We hope to use the system to study the effects of hypoxia and low nutrition concentrations on cancer local invasion and intravasation, two critical steps in early metastasis. Such in vitro models allow quantitative analysis of cell behaviors under precisely controlled cellular environment, which could generate valuable information for the study of specific microenvironmental factors.

The design of the microfluidic device includes two main compartments: a cancer compartment connected with an endothelial channel, which mimics a blood vessel. In the cancer compartment, cancer cells were encapsulated in collagen hydrogel, which provided a more physiological relevant environment for cell culture and migration. The main objective of the design was to independently control the chemical concentrations in the two compartments, in particular, the oxygen tension. To accomplish the goal, our design employs two separate flow circuits to supply cell culture media for the two compartments. In order to achieve a better control of the oxygen concentration, the device was made of oxygen impermeable poly (methyl methacrylate).

One device was built and tested. Oxygen reading in the two compartments and fluorescent dye diffusion test indicate that we could independently control the concentrations of oxygen and other soluble molecules in the two compartments. Cancer cell and endothelial seeding were attempted. Due to time constraints, co-culture experiments were not performed in this project. In summary, we successfully developed and tested a microfluidic system that is suitable for the study of cancer metastasis under different oxygen and nutrition concentrations.

Keywords: microfluidics, tumor microenvironment, cancer metastasis

Preface

This thesis fulfills part of the requirements for the master's degree in the department of biomedical engineering at the Johns Hopkins University. The project was supervised and sponsored by Dr. Sharon Gerecht in the Institute for NanoBioTechnology.

I would like to thank Dr. Sharon Gerecht, Dr. Feilim MacGabhann and Dr. Zachary Gagnon for their support and guidance. In addition, I would like to give my special thanks to Andrew Wang from the Searson Lab, who has provided many insightful suggestions. In particular, Andrew offered important advice on endothelial cell seeding and helped with the Lucifer yellow gradient testing. I also wish to thank John Jameson and Quinton Smith for their valuable help in this project, and Alexander de la Vega and Kevin Zhang for proofreading of the draft.

Table of Contents

1. Introduction	1
1.1 Background	1
1.2 Project Objective	2
1.3 Significance	2
2. Design of the Microfluidic System	4
2.1 Microfluidic Chip Design	4
2.1.1 Device Layout.....	4
2.1.2 Concentration Control.....	5
2.1.3 Flow System Design.....	6
2.1.4 COMSOL Simulation.....	8
2.1.5 Device Material.....	15
2.1.6 Device Fabrication.....	15
3. Microfluidic System Operation	16
3.1 Cell Line and Cell Culture	16
3.2 Device Assembly Using Wax Bonding	16
3.2.1 Bonding Procedure.....	16
3.2.2 Bond Strength Testing.....	18
3.3 System Setup and Sterilization	20
3.3 Flow Rate	20
3.4 Hydrogel Injection and Cancer Cell Seeding	21
3.5 Endothelial Cell Seeding	22
4. Device Characterization	23
4.1 Oxygen Reading	23
4.1.1 Experiment Procedure.....	23
4.1.2 Acellular Oxygen Reading.....	24
4.1.3 Oxygen Reading with Cancer Cells.....	25
4.2 Experimental Characterization of Concentration Gradient	26
4.2.1 Experiment Procedure.....	26
4.2.2 Results.....	27
4.3 HUVEC Cell Seeding	28
4.3.1 Evaluation.....	28
4.3.2 Results.....	29
5. Discussion	32
5.1 Overview	32
5.2 Flow System and Concentration Control	32
5.3 HUVEC Seeding	33
5.4 Future Remarks	34
Citation	36

List of Figures

Figure 1. Design concept development.	3
Figure 2. Schematics showing the design of the microfluidic device.	4
Figure 3. The developed microfluidic device.	5
Figure 4. Schematic depiction of the flow system.	7
Figure 5. Complete flow system setup.....	7
Figure 6. Oxygen and glucose concentration simulations results.....	10
Figure 7. 3D simulation results of the oxygen concentration profiles.	11
Figure 8. 3D simulation results of the glucose concentration profiles.....	12
Figure 9. Diffusion coefficient sensitivity analysis results.....	14
Figure 10. Cancer consumption rate sensitivity analysis results.....	14
Figure 11. Device operation flow chart.....	16
Figure 12. 3D drawing showing device assembly and tube connection.....	17
Figure 13. Wax Bonding.	18
Figure 14. Comparison of bond strength.....	19
Figure 15. Cancer compartment hydrogel injection.....	22
Figure 16. Oxygen sensor placements in the device.	23
Figure 18. Oxygen reading with cancer cells cultured in the cancer compartment.	25
Figure 19: Fluorescent images of Lucifer yellow gradient across the gap channel.	27
Figure 20. Concentration profiles generated based on the fluorescent intensity.	28
Figure 21. EC channel bright-field images.	30
Figure 22. EC channel live and dead staining.	31

1. Introduction

1.1 Background

Despite the significant achievements made in cancer research, cancer is still one of the leading causes of death, and metastasis is primarily responsible for deaths resulting from cancer (1). Local invasion and intravasation are two critical steps in early metastasis, and it is widely acknowledged that the tumor microenvironment has profound effects on a cancer cell's ability to invade its surroundings and cross the endothelial barrier. A better understanding of the interactions between cancer cells and the microenvironment is necessary for the development of effective treatments to combat metastasis.

Because of its poor vasculature, the microenvironment in solid tumors is often characterized by low oxygen and nutrition concentrations, which have been shown to regulate pathways that are involved in metastasis (2-4). For example, hypoxia up-regulates the expression of HIF-1, which promotes cancer invasion through some of the downstream pathways including Notch and TGF- β (5). Passive diffusion and cell consumption also create various chemical gradients that promote cancer cell migration and invasion (6). However, the exact roles of the altered oxygen and nutrition concentrations and gradients in cancer invasion and intravasation are still unclear.

Technologies that allow for direct observation of cancer cell behaviors under precisely controlled chemical concentrations and gradients would be helpful in generating new knowledge about how these critical environmental factors drive cancer invasion and intravasation. Microfluidic systems allow accurate control and easy manipulation of the cell culture environment. In addition, cell behaviors could be observed and recorded using time-

lapse microscopy. To better understand the specific roles of various concentrations and gradients in cancer progression, there is a need for the development of better microfluidic systems for the study of cancer metastasis.

1.2 Project Objective

In this project, I aim to develop a microfluidic system that is suitable for the study of the effects of low oxygen and nutrition concentrations on cancer local invasion and intravasation. The device is a cancer - endothelial co-culture microfluidic device that simulates the tumor microenvironment and tumor-vascular interface, and it allows precise control of the chemical concentrations and gradients experienced by cancer cells independent of the endothelial cells. A key objective of the project involves controlling the oxygen concentration and gradient within the device. Although there are designs to control concentrations and gradients of soluble molecules, current designs are inefficient in controlling concentrations and difficult to operate. Besides oxygen, other soluble molecules could be studied using the device. In this study, we will focus on controlling the concentration of glucose, an important nutrient, as an example.

1.3 Significance

The microfluidic device developed in this project allows for real-time imaging and quantification of cell behaviors under precisely controlled chemical concentrations and gradients. Such technology would be useful in understanding the effects of specific microenvironmental factors in promoting cancer metastasis. In addition, in vitro models are important for the parameterization and validation of computational models, an area that has

garnered increasing interest in biomedical research. In vitro models allow parameters to be measured under well-controlled conditions, and can generate necessary input parameters for computational models. In vitro models are also excellent platforms for experimentally validating simulations. The microfluidic device developed in this project has the potential to assist in the development of computational models, which would play a key role in the study of the tumor microenvironment in the future.

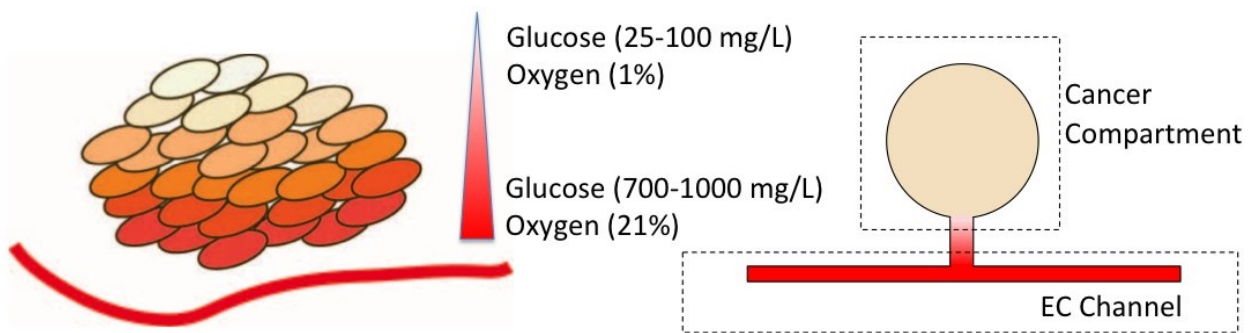


Figure 1. Design concept development. The device mimics the situation of cancer cells adjacent to a blood vessel, and we aim to independently control the oxygen and nutrition concentrations in the cancer compartment and test their effects on cancer cell invasion and intravasation.

2. Design of the Microfluidic System

2.1 Microfluidic Chip Design

2.1.1 Device Layout

To simulate the process of cancer invasion and intravasation, the device consists of two main compartments, the endothelial channel and the cancer compartment, connected by two small gap channels (**Figure 2 & 3**). The cancer compartment and the gap channels are filled with ECM hydrogel, providing a more physiologically relevant environment for cancer cells. The endothelial channel is seeded with endothelial cells to mimic a blood vessel. To simulate intravasation, the model requires a continuous endothelial monolayer at the hydrogel – EC channel interface. The design allows direct observation of cancer cells migrating and crossing the endothelial barrier under different chemical concentrations and gradients across the two compartments. Both the EC channel and the gap channels have square cross sections. The width of the EC channel is 250 μm , and the width of the gap channel is 175 μm .

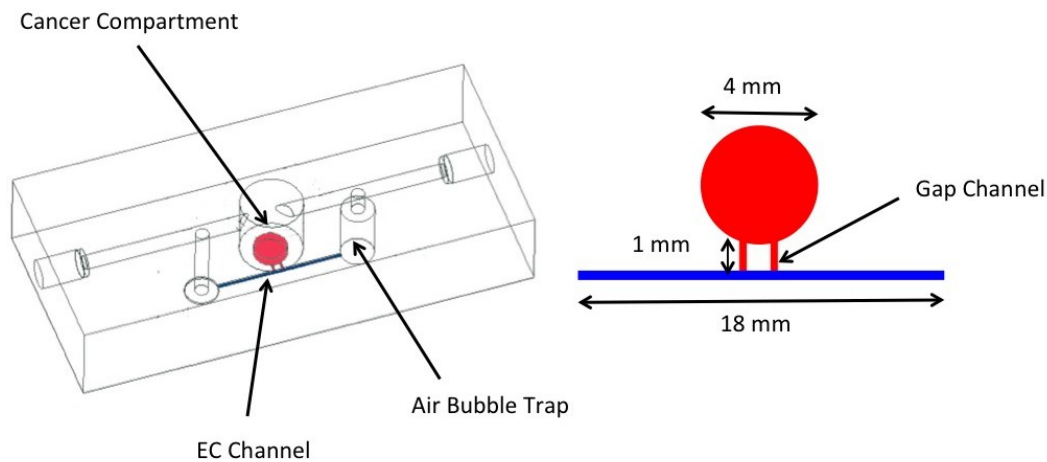


Figure 2. Schematics showing the design of the microfluidic device. Red: cancer compartment and gap channels. Blue: EC channel.

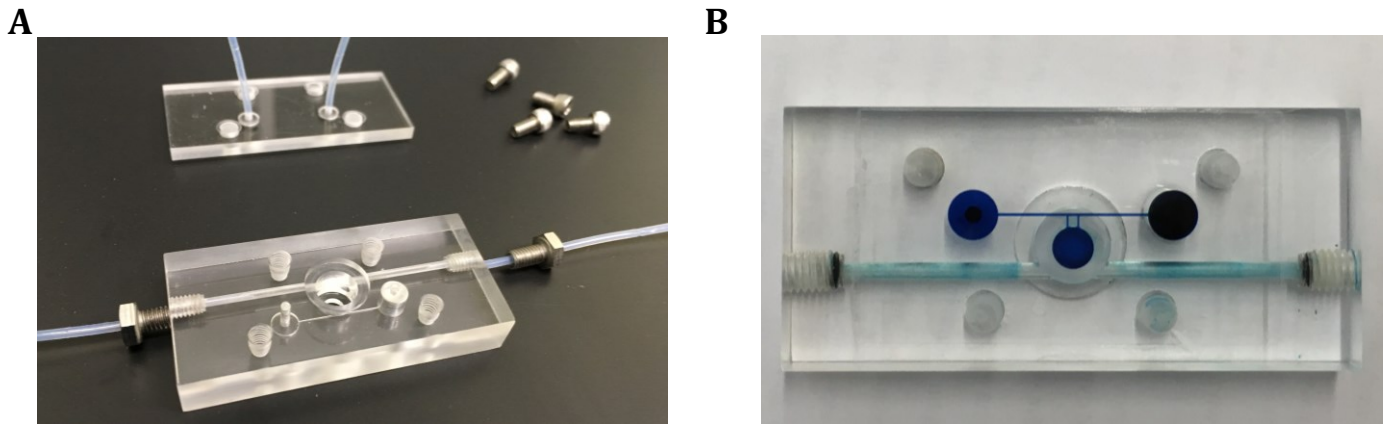


Figure 3. The developed microfluidic device. A) Device and cap partially connected with the tubing. B) Channels filled with blue dye

2.1.2 Concentration Control

The device would be used to test whether important characteristics in the tumor environment, such as a low oxygen concentration and gradient, could promote cancer invasion and intravasation. To fulfill the goal, we need to be able to vary the concentrations in the cancer compartment while maintaining a consistent environment in the EC channel in different experiments.

To independently control and maintain the chemical concentrations in the two compartments, cell culture media is supplied by a circulating system powered by a peristaltic pump. Each compartment has its own circuit, and can be filled with media of different compositions, such as varying glucose concentrations. With different concentrations in the cancer compartment and EC channel, a concentration gradient can be generated across the gap channel, mimicking the gradient commonly found in solid tumors.

One challenge in this design involves controlling the device's oxygen concentration. Microfluidic devices are generally made of polydimethylsiloxane (PDMS), which is highly

oxygen permeable. As a result, it is very difficult to independently control oxygen concentrations in the cancer compartment without interfering with the EC channel. Current designs utilize additional gas channels placed at different locations to generate oxygen gradients across the device. Such methods are inefficient, and the complexity of the design makes the device difficult to use, resulting in limited experimental usage (7). Using oxygen impermeable materials instead of PDMS would allow better control over oxygen concentrations in individual compartments. Hypoxia could be achieved by deoxygenating the media in an external media reservoir before flowing media into the device.

2.1.3 Flow System Design

The flow system consists of two independent flow circuits powered by one peristaltic pump (**Figure 4 & 5**). There are two kinds of tubing. Because of the need to maintain low oxygen concentration in the cancer compartment, the flow circuit uses oxygen impermeable PTFE tubing (Cole-Parmer Instrument, Vernon Hills, IL). The endothelial channel circuit uses softer oxygen permeable tubing.

Each flow circuit has its own media reservoir. Cancer media is directly deoxygenated inside the media reservoir, which is made of oxygen impermeable PMMA. To deoxygenate the media, gas containing 1% oxygen, 5% carbon dioxide 74% nitrogen was bubbled through the media in the reservoir. As the device and tubing for the tumor circulation system are in theory oxygen impermeable, the media remains deoxygenated when it reaches the cancer compartment. Oxygen concentration could then be modified by flowing gas with different oxygen concentrations. The design allows for easy and reliable control of the oxygen concentration and other chemical concentrations in the device.

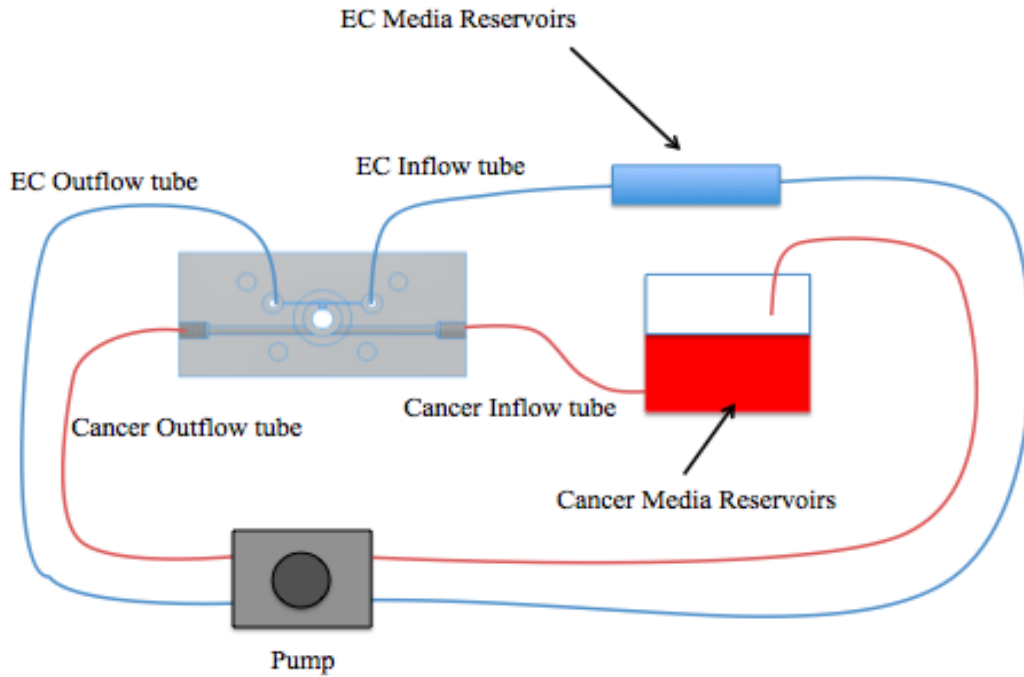


Figure 4. Schematic depiction of the flow system. The system includes two separate flow systems for each compartment, allowing independent control over the chemical concentrations.

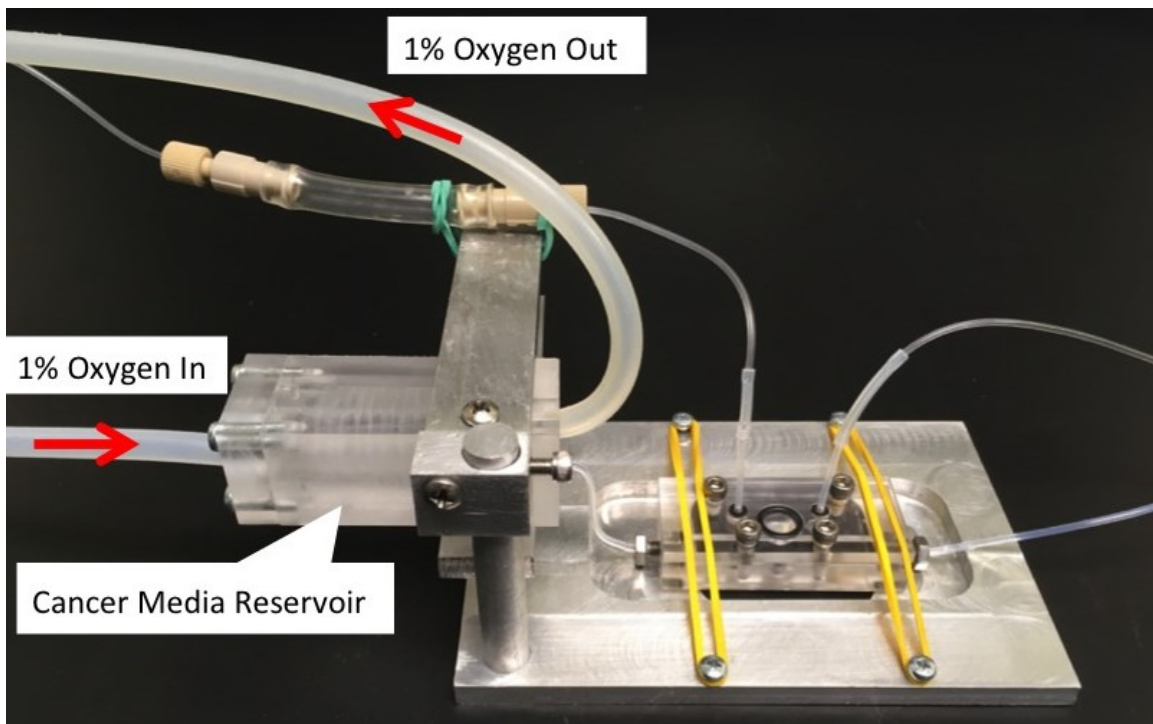


Figure 5. Complete flow system setup

2.1.4 COMSOL Simulation

To evaluate whether we could generate desired oxygen concentration profiles with the designed microfluidic system, steady state oxygen concentrations in the device were simulated using finite element analysis software COMSOL Multiphysics 5.1 (COMSOL, MA, USA). In addition, concentration profiles of another important soluble molecule, glucose, are simulated.

The simulations were based on COMSOL transport of diluted species. All transport parameters, such as oxygen diffusion coefficients in collagen, were obtained from the literature (8-11). The cancer cell line we used for the project was $Kras^{G12D/+}$, $Ink4a/Arf^{fl/fl}$ (KIA) mouse sarcoma cells, and the endothelial cell line was Human Umbilical Vein Endothelial Cells. The HUVEC glucose and oxygen uptake rates were obtained from Abaci et al and Guzzardi et al respectively. Since the oxygen and glucose concentrations in the EC channel are much higher than the Michaelis-Menten constant, we assumed the consumption rate to be zero order. KIA cell oxygen and glucose consumption rates were not available, so we estimated the values from normal cells (12). Oxygen consumption rates were modeled using Michaelis-Menten kinetics, and glucose consumption is modeled as first order (13, 14). To test the affects of cancer consumption variation on the concentration profiles, I perform a sensitivity analysis by perturbing cell consumption rates and diffusion coefficients.

The KIA cell density in the cancer compartment was 1.5×10^6 cells / ml. In the simulation, it was assumed HUVECs were confluent on all sides of the EC channel, and that the cell density was 4.5×10^5 cells / cm^2 (10). It should be noted that the model only requires a HUVEC monolayer at the gel interface, and that HUVECs do not have to cover all four

sides throughout the entire channel. Our simulation tested a situation of maximum oxygen and glucose consumption in the EC channel.

Parameter	Value	Reference
Oxygen diffusion coefficient in media	$3.35 \times 10^{-5} \text{ cm}^2 / \text{sec}$	10
Oxygen diffusion coefficient in collagen	$1.7 \times 10^{-6} \text{ cm}^2 / \text{sec}$	8
Desired oxygen level in EC channel	0.22 mmol / L	N/A
Desired oxygen level in the cancer compartment	0.1 mmol / L	N/A
HUVEC oxygen consumption rate per cell	10^{-17} mol/sec	10
Cancer O2 consumption baseline V_{\max}	$2.5 \times 10^{-18} \text{ mol / sec}$	13
Cancer O2 consumption baseline K_m	10^{-6} mol / L	13
Glucose diffusion coefficient in collagen	$1.3 \times 10^{-6} \text{ cm}^2 / \text{sec}$	9
Glucose diffusion coefficient in media	$5.67 \times 10^{-6} \text{ cm}^2 / \text{sec}$	11
Desired glucose concentration in EC channel	1000 mg / L	N/A
Desired glucose concentration in the cancer compartment	100 mg / L	N/A
HUVEC glucose consumption rate per cell	$3.47 \times 10^{-14} \text{ g/sec}$	11
Cancer baseline glucose consumption coefficient	$5.42 \times 10^{-13} \text{ g/sec}$	14

Table 1: Parameters used in COMSOL Modeling

We assumed that the flow system could effectively maintain the chemical concentrations in the media above the cancer compartment, and we set a constant concentration boundary on the top surface of the hydrogel in the cancer compartment. We assumed that there was no flow in the gap channel, and molecular transport is solely through diffusion. The flow rate in all the simulations was set to be 5 ml / hr.

Percent oxygen entering the EC channel was 21% and the glucose concentration was 1000 mg/L respectively, which is the concentration in common endothelial cell media. In the cancer compartment, inflow media with 1% oxygen, 21% oxygen, 100mg/L glucose and 1000mg/L glucose were simulated.

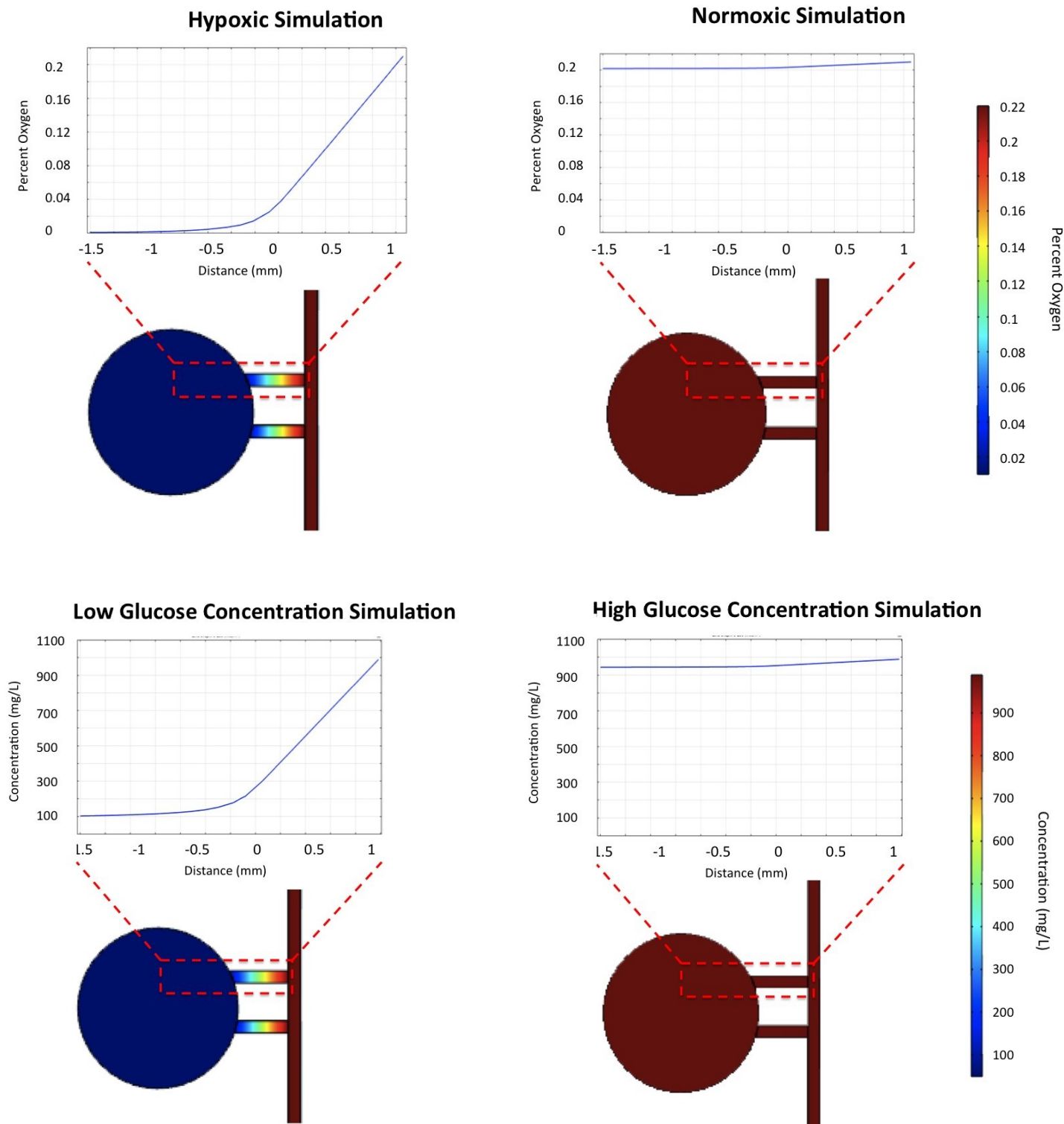


Figure 6. Oxygen and glucose concentration simulation results. Based on the simulation, the flow system design could effectively control the concentrations in the cancer compartment. Under hypoxic and low glucose experimental settings, linear concentration gradients were formed along the gap channel.

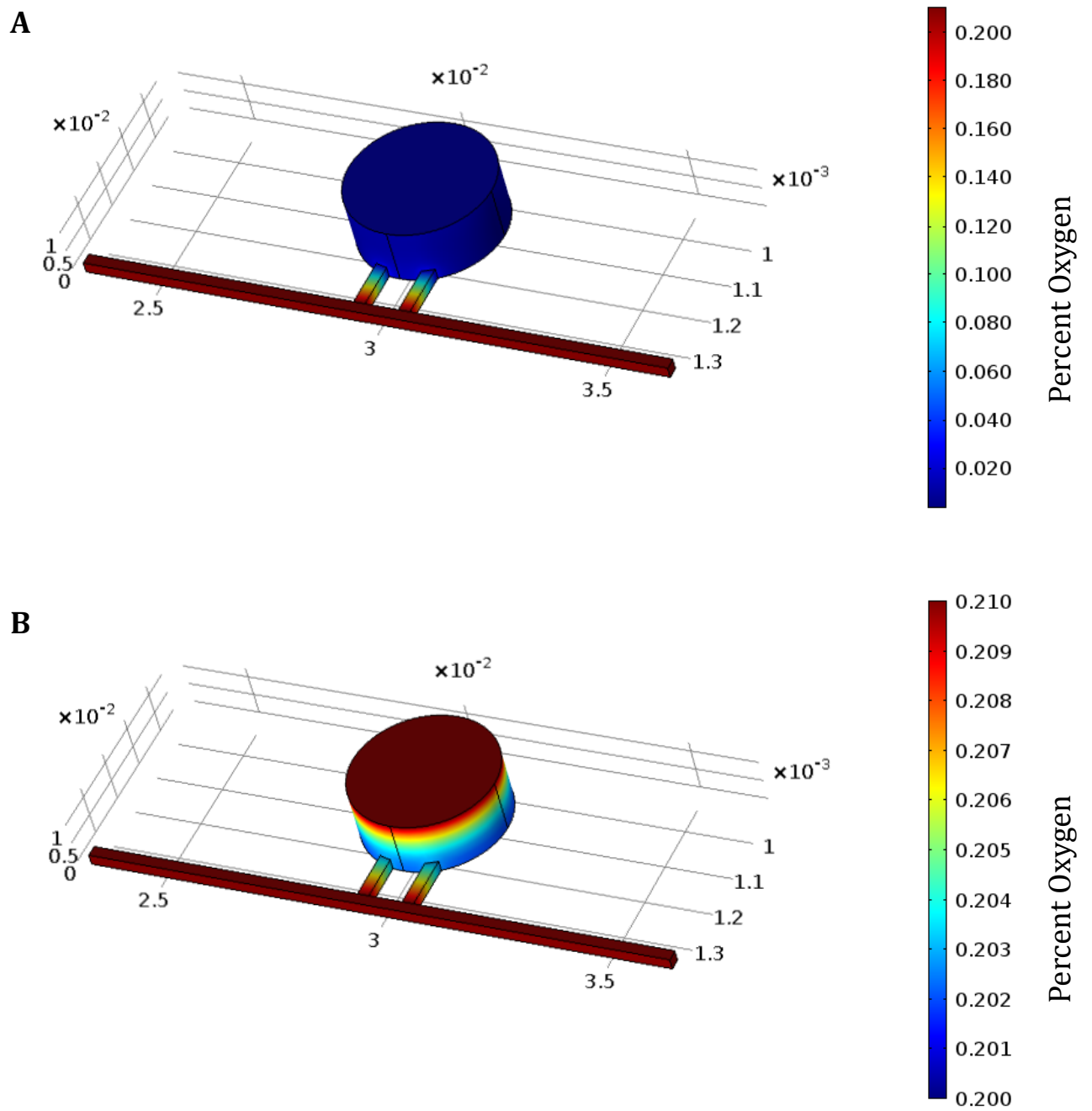


Figure 7. 3D simulation results of the oxygen concentration profiles. **A)** Hypoxic experiment setting. **B)** Normoxic experiment setting. The color bars in each panel span different ranges.

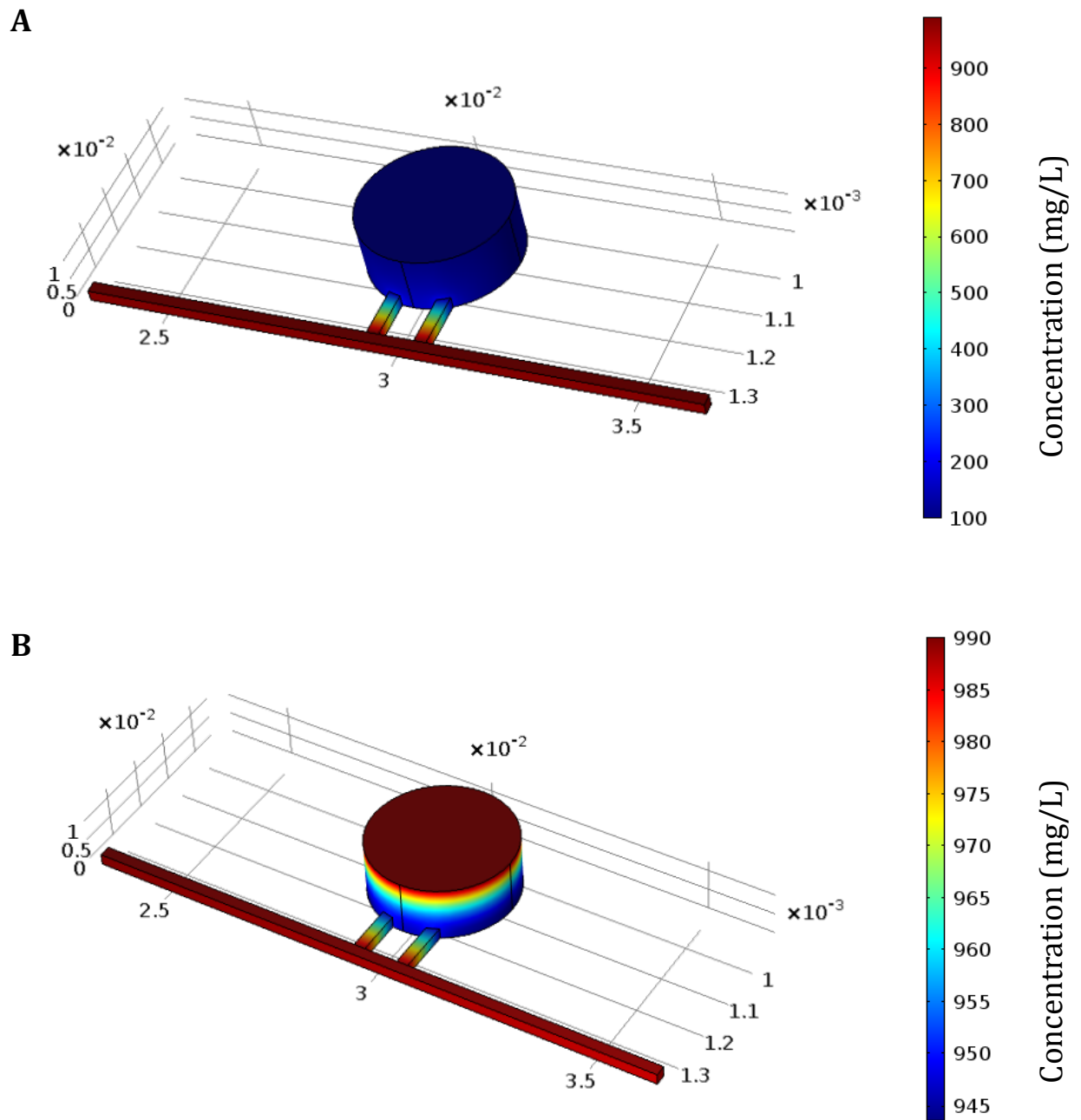


Figure 8. 3D simulation results of the glucose concentration profiles. **A)** Low glucose concentration experiment setting. **B)** High glucose concentration experiment setting. The color bars in each panel span different ranges.

Results from the simulations are shown in figure 6 - 8. As expected, under low glucose and hypoxic conditions, the concentrations in the gap channel decrease linearly, and the concentrations in the cancer compartment is very close to the concentrations we aim to achieve. The simulation results indicate that with two independent flow circuits, we could control the chemical concentrations in the cancer compartment without interfering with the EC channel and generate the desired gradients.

Diffusion coefficients of the hydrogel could vary from the literature value, and oxygen and glucose consumption rates of KIA cancer cells are not available. To test the robustness of the assumed values for these parameters, I performed a sensitivity analysis on the oxygen and glucose diffusion coefficients in collagen, and on cancer oxygen and glucose consumption rates. The analysis involves comparing the concentration profile along the gap channel by varying one parameter at a time. Results are shown in figure 9 and 10. Modifying oxygen and glucose diffusion coefficients has a very small effect on the concentration profiles with respect to the control. Under low glucose and hypoxic conditions, a tenfold increase or decrease in these values still produces concentrations within the hypoxic and low glucose range in the cancer compartment. Changing the oxygen consumption rate by 50% does not result in large differences. Since cancer cells are known to have a high glucose consumption rate, we increased the consumption rate by ten times. This caused a small decrease in the concentration in the cancer compartment. Decreasing glucose consumption has almost no effects on the concentration profile.

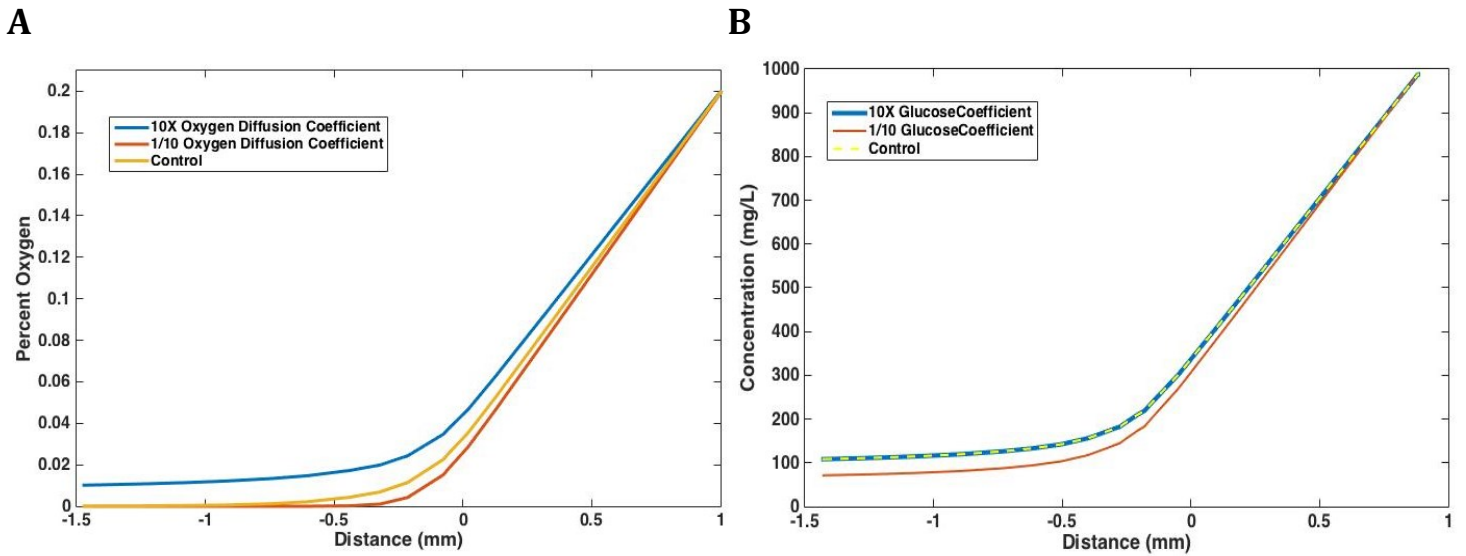


Figure 9. Diffusion coefficient sensitivity analysis results: **A)** Oxygen concentration profiles along the gap channel with 10 fold perturbation in oxygen diffusion coefficients. **B)** Glucose concentration profiles along the gap channel with 10 fold perturbation in glucose diffusion coefficients.

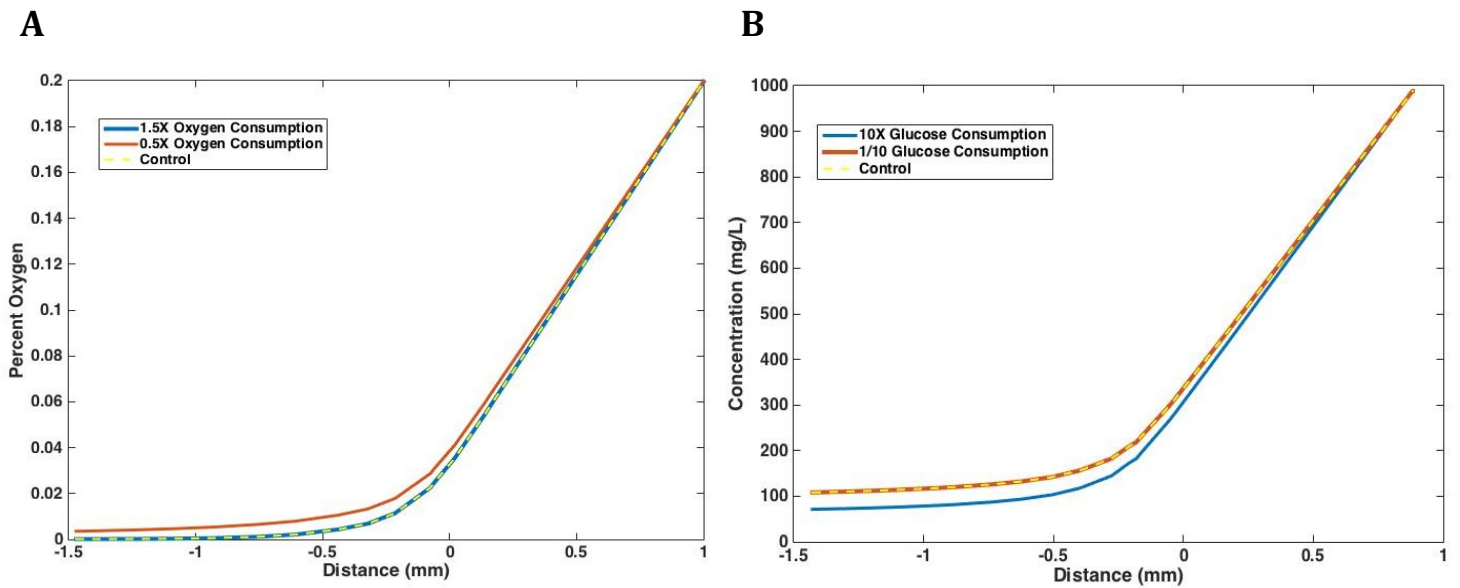


Figure 10. Cancer consumption rate sensitivity analysis results: **A)** Oxygen concentration profiles along the gap channel with 50% perturbation in oxygen consumption rate. **B)** Glucose concentration profiles along the gap channel with 10 fold perturbation in glucose consumption.

2.1.5 Device Material

There are many oxygen impermeable materials that are available, such as poly (methyl methacrylate) (PMMA) and poly carbonate. PMMA was chosen to be the material for the device because of its mechanical strength and resistance to scratching. In addition, PMMA is transparent, allowing for easier observation.

The top opening of the device is sealed with a PMMA cap secured by four screws at the four corners. Tubings are connected to the device using O-ring boss seals.

2.1.6 Device Fabrication

The CAD model of the microfluidic device was designed using Autodesk Inventor (Autodesk, San Rafael, CA, USA). PMMA blocks and O-rings were purchased from McMaster Carr, Santa Fe Springs, CA. The device was built in the Wyman machine shop at the Johns Hopkins University.

3. Microfluidic System Operation

3.1 Cell Line and Cell Culture:

Human Umbilical Vein Endothelial Cells (HUVEC) were cultured in endothelial growth medium (PromoCell, Heidelberg, Germany). HUVECs were passaged every 3 to 5 days using 0.05% trypsin. HUVECs used in experiments were either passage 4 or passage 5.

$Kras^{G12D/+}$, $Ink4a/Arf^{fl/fl}$ (KIA) mouse sarcoma cells were cultured in Dulbecco's Modified Eagle Medium (DMEM) with 10% FBS and 1% penicillin. KIA cells were passaged using 0.25% trypsin.

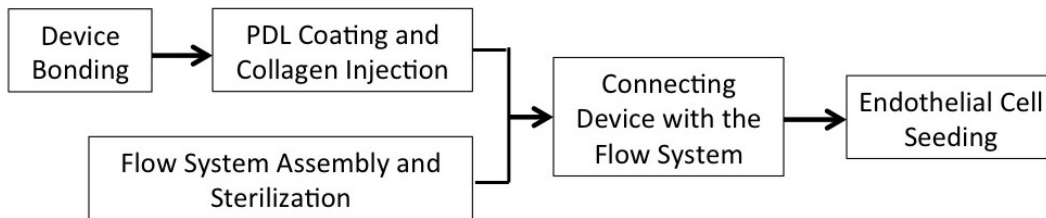


Figure 11. Device operation flow chart

3.2 Device Assembly Using Wax Bonding

3.2.1 Bonding Procedure

Currently, there are very few bonding methods available to bond PMMA and glass, and most of them require special equipment. In addition, the price of constructing our PMMA device is very high. In order for the device to be economically practical for laboratory research, the

bonding needs to be reversible, so that the device could be reused. Gong et al. reported using wax to bond PMMA microfluidic devices, which was used for this project (15).

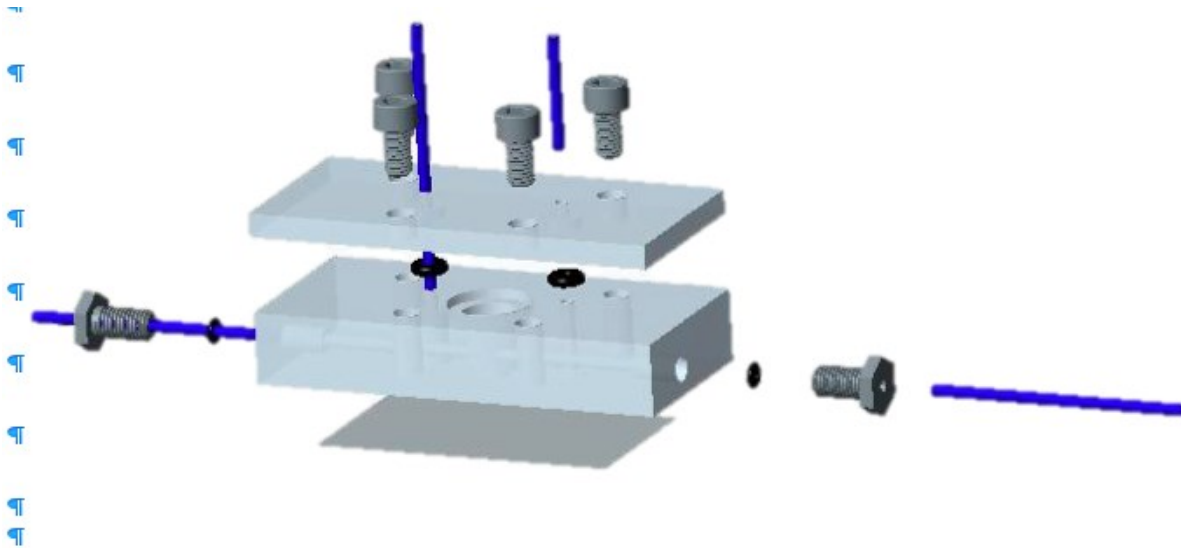


Figure 12. 3D drawing showing device assembly and tube connection. The glass slide was bonded with the device using wax and the tubings are secured with O-ring boss seals.

Following the ideas reported by Gong et al, we developed the following protocol. Before assembly, the bottom surface of the device was cleaned with ethanol and small particles on the surface were removed using Scotch tape. Wax was melted at 80C. The bottom surface of the device was immersed in wax and attached to a glass cover slide. At this point, all channels were clogged with wax, which would need to be removed before the device could be used. To clean the wax, the device was first clamped tightly by a special metal scaffold in order to protect the wax layer between the device and glass (**Figure 13A**). The device was then placed in an 80 C hot water bath, and wax inside the channels was removed through washing with soap. The device was then allowed to cool down slowly. Afterwards, soap

water remaining the device was cleared with DI water and ethanol. Bright-field image of the channel after removal of wax is shown in figure 13B. The bonding could be easily reversed by melting the wax at 80 C, allowing the microfluidic device to be reused.

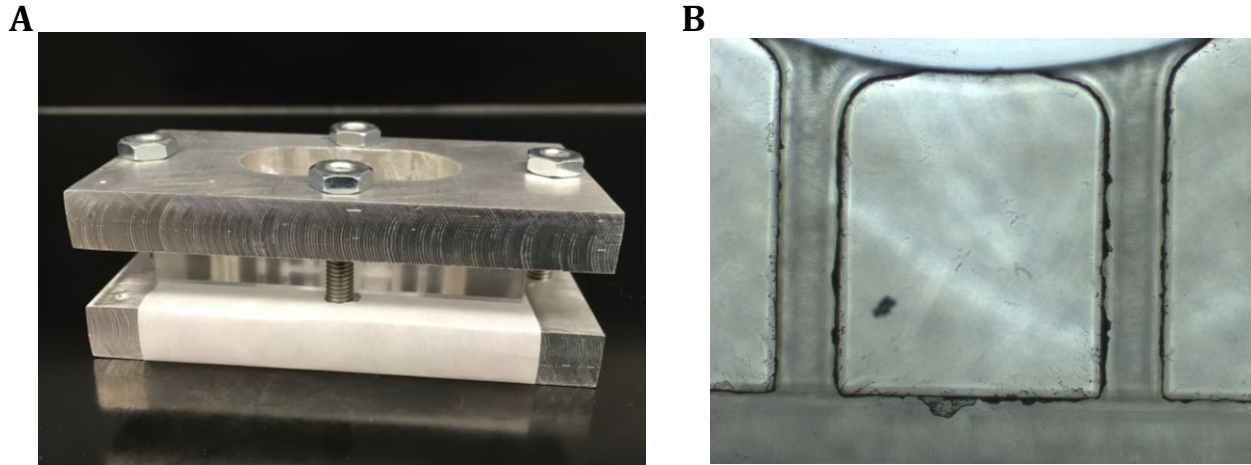


Figure 13. Wax Bonding. **A)** Device clamped by the metal scaffold before removing wax in the hot water bath. **B)** 4X microscope images of the gap channels after wax removal.

3.2.2 Bond Strength Testing

The bond strength between the glass and the PMMA device was assessed using burst pressure test. The top of the device was sealed with a piece of glass slide using vacuum grease. One side of the cancer media channel was attached to pressurized gas source and the other side was sealed. Gas pressure was steadily increased to determine the burst pressure the device could withstand. In the three trials performed, average burst pressure was 0.063 mPa, and the standard deviation was 0.011 (**Figure 14**). Our bonding strength is comparable to that of other reversible bonding techniques, such as magnetic clamping (16, 17). In general,

reversible bonding is much weaker than irreversible bonding techniques such as PDMS plasma bonding (18). The bonding strength provided by wax is sufficient for the purpose of this project. Only one device was created, and it was still functioning by the end of the project, demonstrating the reversibility of this bonding method. PMMA has many advantages over PDMS. Besides its low oxygen permeability, PMMA additionally benefits from lower vapor permeability. Its rigidity and machinability also allow for more complex 3D structures. The lack of easy bonding techniques is one of the hurdles that prevent people from using PMMA for microfluidic fabrication. With wax bonding, PMMA would be able to play a more important role in the creation of microfluidic devices.

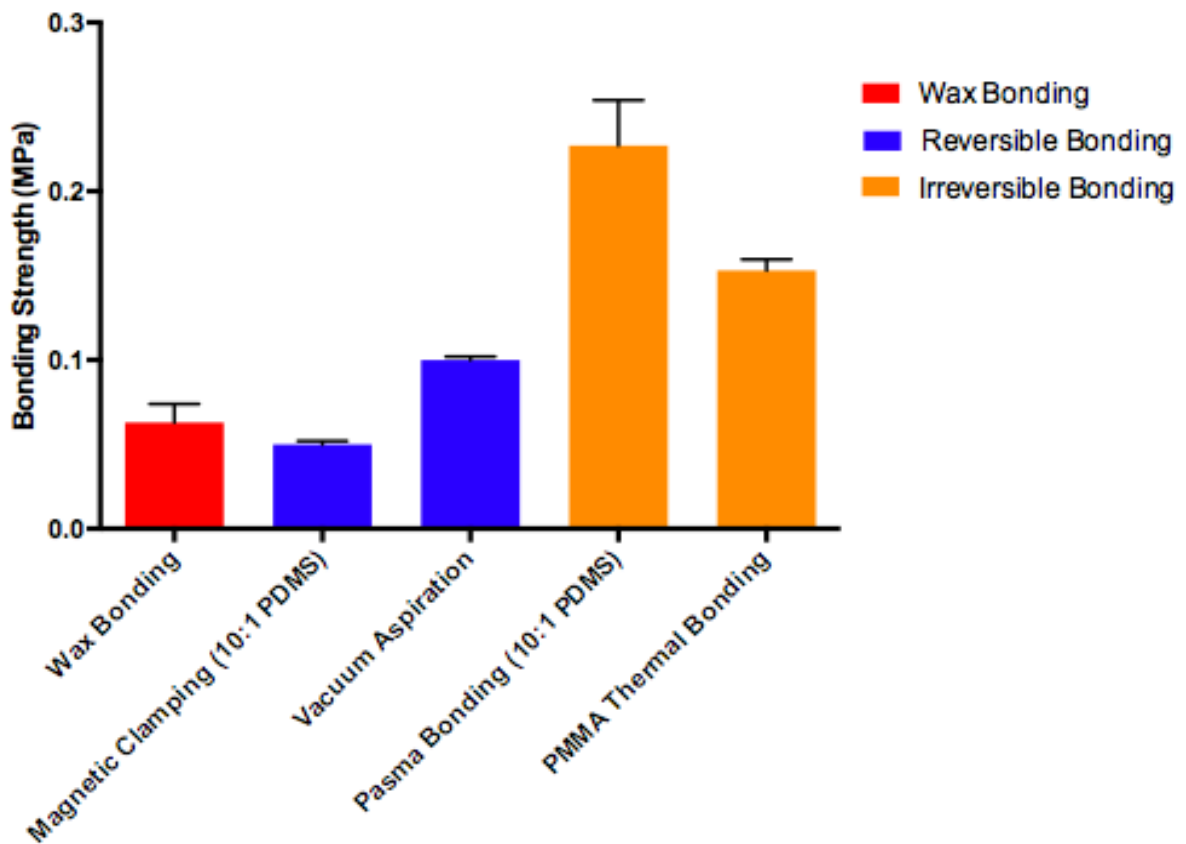


Figure 14. Comparison of bond strength. Our wax bonding strength is similar to other reversible bonding methods. Although it is lower than permanent bonding methods, such as PMMA thermal bonding, the strength is sufficient for the purpose of this project.

3.3 System Setup and Sterilization

Reservoirs, tubing and the pump are first connected and assembled in a cell culture hood and sterilized by flowing 100% ethanol through the system for 5 minutes. Ethanol is then aspirated and any remaining ethanol is allowed to evaporate in a hood for at least 3 hours. Complete experiment procedure is shown in figure 11, and tubing attachment on the device is shown in figure 12.

3.3 Flow Rate

Media flow rate is one of the important parameters that need to be determined, and there are many factors that must to be considered when determining the flow rate of the system.

First of all, the flow rate should be sufficient to provide enough oxygen and nutrition to the cells. Minimum flow rate required to support HUVEC cells inside the EC channel was calculated based on simple mass balance. $Q_{\min} = R * n / \Delta C$, where n is the number of cells and ΔC is the concentration difference between the inlet and outlet. Ideally, the oxygen concentration difference between the inlet and outlet should be less than 5 mmol / L, and the glucose concentration difference should be less than 50 mg/L. The calculated flow rate based on oxygen consumption is 0.5 ml / hr, and the calculated flow rate based on glucose consumption is 0.16 ml / hr.

When designing the microfluidic system, we assumed the system to be completely oxygen impermeable. However, there will always be small oxygen exchanges between the system and the surroundings, such as leaks at the tube connections. As a result, the system would require the flow rate to be above a minimum value in order to counter oxygen

exchange with the external environment and maintain a low oxygen level in the cancer compartment.

Another factor that needs to be considered is the pressure imbalance between the EC channel and the cancer compartment, which will result in liquid flow between the two compartments through the gap channels. The flow generated by peristaltic pumps is pulsed. Since both flow circuits are powered by a single peristaltic pump, a high flow rate would result in a large inter-compartmental flow, affecting concentration profiles and cell behaviors.

Considering all the factors mentioned above, the final flow rate is set to be 5 ml per hour.

3.4 Hydrogel Injection and Cancer Cell Seeding

In order to provide a more physiological relevant environment for cancer cell culture and migration, the cancer compartment and the gap channels were filled with type I collagen. To improve the attachment of collagen to PMMA, the device was coated with 1 mg/L poly D lysine (PDL) (Sigma-Aldrich, St Louis, MO) at 37 C for 10 hours, and further dried at 37 C for another 12 hours. The device was then washed three times using DI water. Rat Tail Type I Collagen (Corning, Midland, MI, USA) was used to form the hydrogel scaffold. Collagen was made following a protocol established by Nguyen-Ngoc et al (19). After mixing, 5 μ l of collagen without cells was injected directly from the cancer well into the gap channel. 8 μ l of collagen with cancer cells was then introduced into the cancer compartment, and was mixed with previously injected collagen inside the cancer compartment (**Figure 15**). The device was placed in a humidified cell culture incubator for 45 minutes to allow gelation.

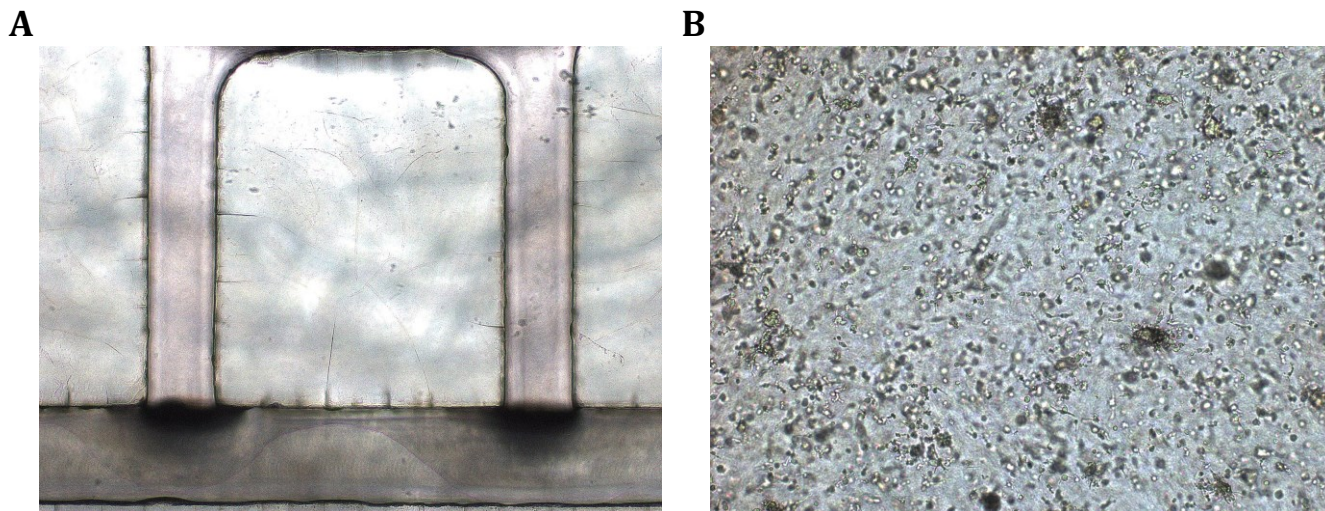


Figure 15. Cancer compartment hydrogel injection. A) Collagen in the gap channels after injection. B) Day 1 bright-field image of KIA cells in the cancer compartment.

3.5 Endothelial Cell Seeding

After cancer cell seeding, HUVEC cells were introduced into the EC channel to generate the tumor-vascular interface. The most successful experiment procedure is reported here, and further evaluation of the seeding protocol is described in section 4.3.

After seeding KIA cells in the cancer compartment, endothelial cells were introduced into the EC channel. Because the device was made of oxygen impermeable PMMA, cells could not obtain oxygen diffused from the external environment, and would need to rely on the limited amount of oxygen present in the cell culture media. As a result, a flow needed to be generated immediately to provide sufficient oxygen for the endothelial cells. In order to minimize the effects on the initial cell attachment, we used a syringe pump to generate a flow going from the EC channel to the cancer compartment. This initial inter-compartmental flow served two purposes: 1) providing oxygen to the endothelial cells, 2) encouraging endothelial

cell attachment at the gel interface. After 1.5 hour, the inter-compartmental flow was stopped and replaced by the circulating flow powered by the peristaltic pump.

4. Device Characterization

4.1 Oxygen Reading

4.1.1 Experiment Procedure

To experimentally test the oxygen concentrations inside the device, oxygen tensions in the two compartments were monitored using fluorescent oxygen sensors (OXY-4 mini, PreSens GmbH, Regensburg, Germany). The sensors were placed inside the device using silicon vacuum grease (Dow Corning, Midland, MI). One sensor was placed in the cancer well, and the other sensor was placed at the outlet of the EC channel (**Figure 16**). The experiments were conducted under a flow rate of 5 ml/hr for a period of 24 hours.

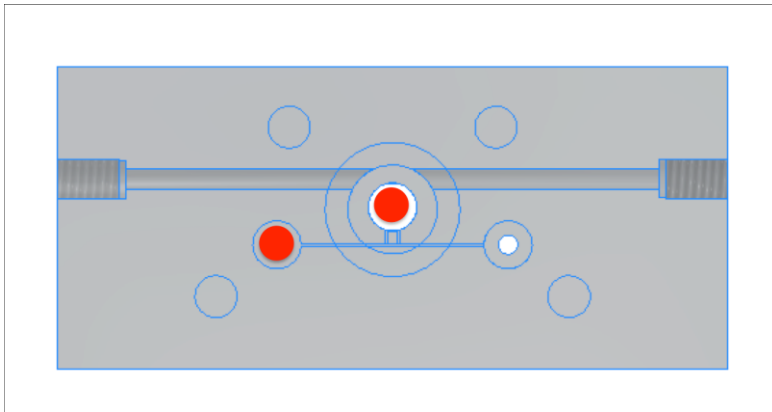


Figure 16. Oxygen sensor placements in the device. The figure shows the top view of the device and the red dots indicate the locations of the sensors.

4.1.2 Acellular Oxygen Reading

To test whether the design could achieve low oxygen level in the cancer compartment while maintaining normoxia in the EC channel, oxygen concentrations in the two compartments were monitored for 24 hours. To test the effectiveness of the flow system in controlling oxygen level, this experiment was conducted without cells in the device. Due to time constrain of the project, this experiment was only repeated twice.

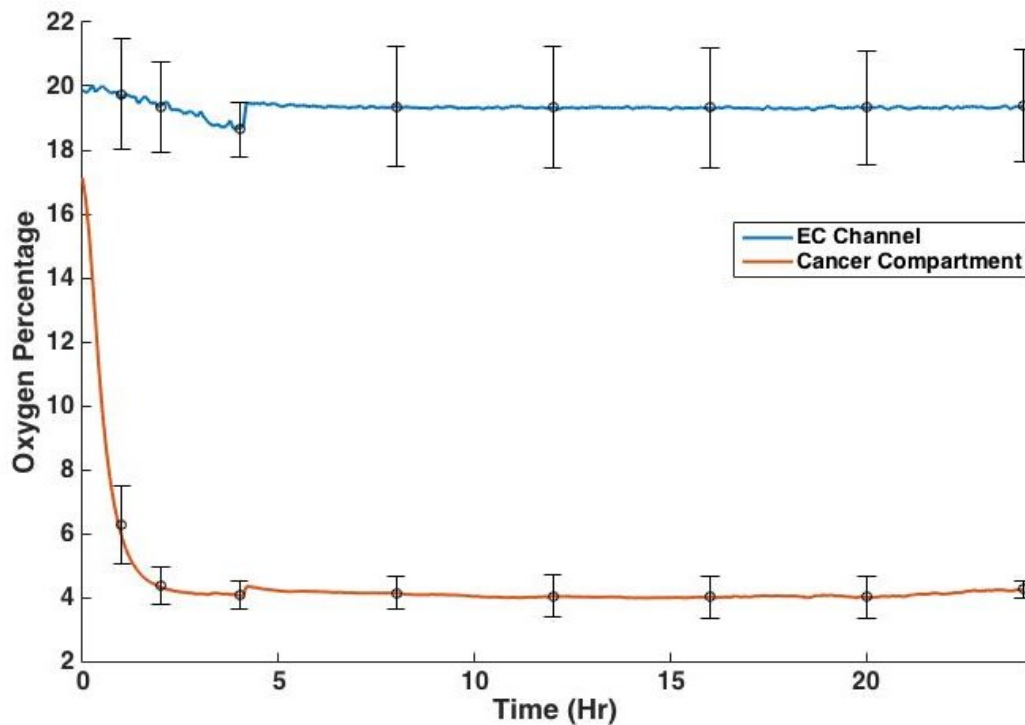


Figure 17. Acellular oxygen reading. The experiment was repeated twice; mean and standard deviation were calculated. Overall, the performance was stable, and the cancer compartment reached below 5% oxygen very quickly. In the future, there is a need to repeat this experiment and further validate the reliability of the flow system design.

The oxygen concentration in the cancer compartment quickly decreased to around four percent, while the concentration in the EC channel stabilized at around 20% (**Figure 17**). The steady state oxygen concentrations in the cancer compartment were higher than the prediction by the COMSOL simulation, which might be caused by small leaks in the system. This experiment would need to be repeated more times in order to further validating the reliability of the flow system design.

4.1.3 Oxygen Reading with Cancer Cells

Cell consumption might affect oxygen control inside the device. With cancer cells encapsulated inside collagen, oxygen concentrations inside the cancer compartment would decrease. To test the effects of cancer cells on oxygen concentrations, oxygen tension was monitored for three days with cancer cells cultured in the cancer compartment

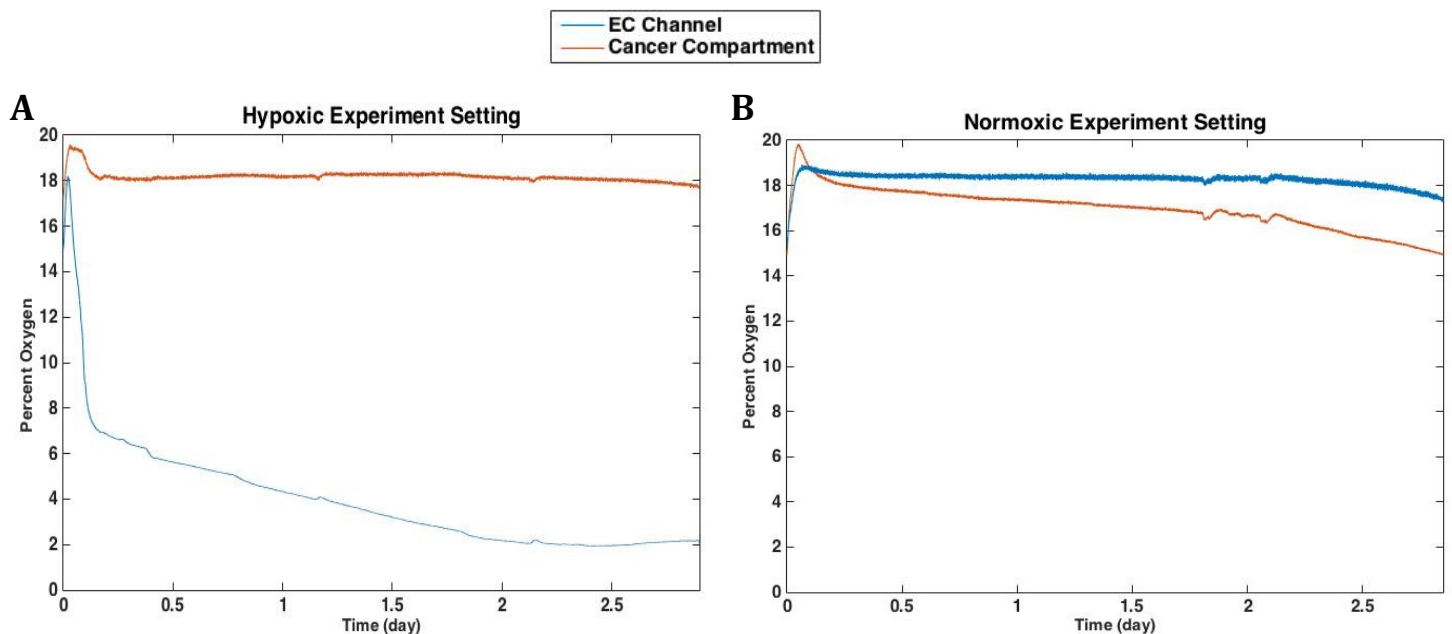


Figure 18. Oxygen reading with cancer cells cultured in the cancer compartment. **A)** Oxygen reading under hypoxic experiment setting. **B)** Oxygen reading under normoxic experiment setting.

Under hypoxia experiment settings, oxygen concentration in the cancer compartment decreased slowly over the first two days, and reached steady state at around 2% oxygen (**Figure 18A**). Under normoxic experimental settings, oxygen concentration decreased gradually over three days to around 15%, which is still within the normoxic range (**Figure 18B**). The results show that the flow system could effectively control the oxygen tension with the presence of cells.

4.2 Experimental Characterization of Concentration Gradient

4.2.1 Experiment Procedure

To experimentally test the concentration gradient formation between the EC channel and the cancer compartment, we introduced a small fluorescent molecule, Lucifer yellow, to the EC channel. The concentrations were measured based on fluorescent intensity. The experiment was performed using a Nikon A1-Rsi confocal microscope with 10X magnification. The wavelength is 405 nm and the exposure time is 400 ms. Images were taken every minute for three hours. For simplicity, we used a basic gravity driven flow system with a flow rate of approximately 3 ml/hr. 1 mM Lucifer yellow was added to the EC reservoir after the flow was established and stabilized. Flow rate was verified at the end of the experiment by measuring the liquid volume in the reservoirs. Images were analyzed using imageJ. Relative concentration plots were graphed in Matlab.

4.2.2 Results

After the introduction of Lucifer yellow, the intensity gradient was observed across the gap channel and reached the steady state in approximately 15 min. The experimental measurements and the COMSOL simulation matched well, although one key difference was the shapes of the profiles across the gap channel. The simulation indicates that concentration profile should be linear. The curved shape in the experimental data might be caused by slow inter-compartmental flow going from the cancer compartment to the EC channel.

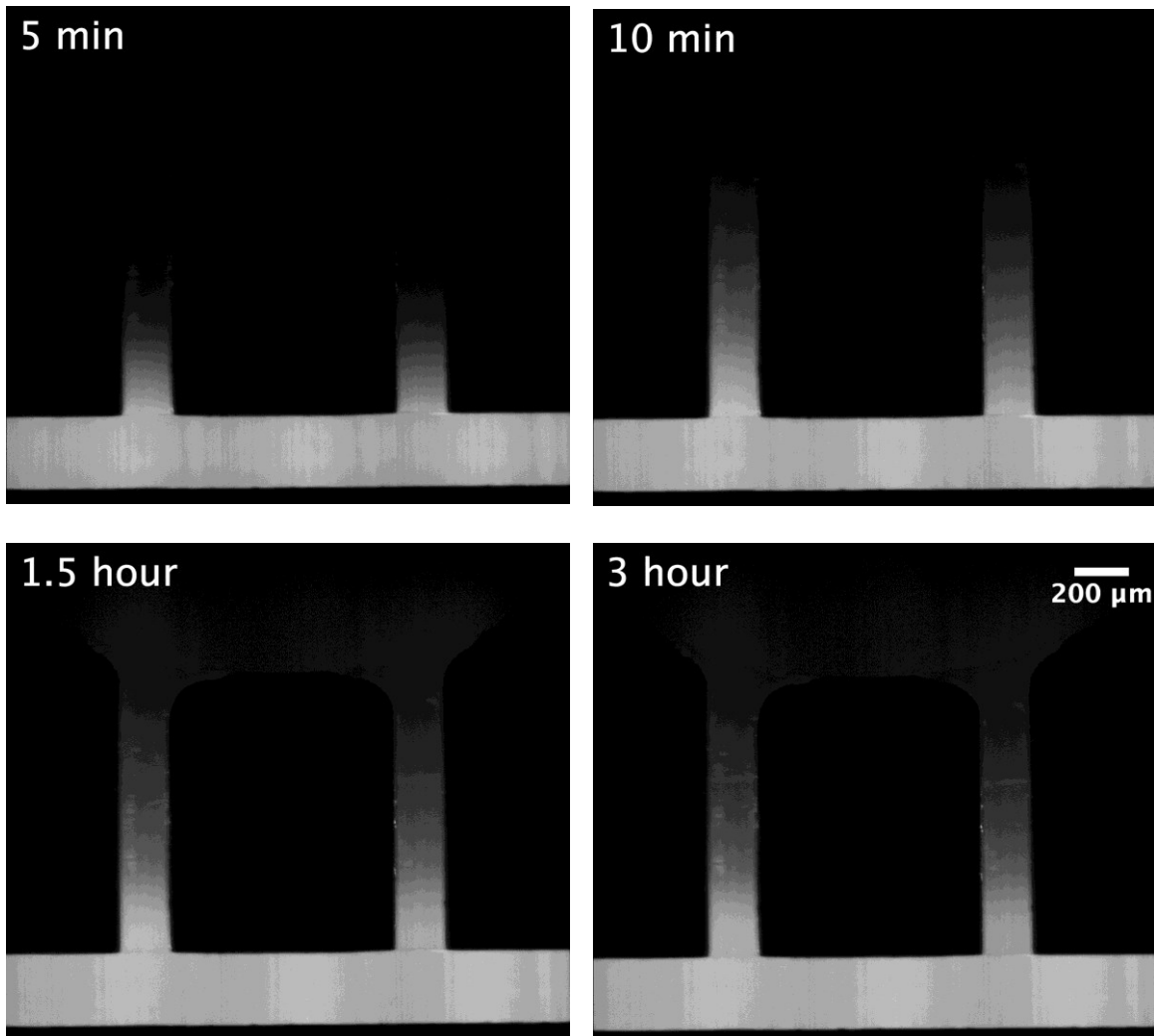


Figure 19: Fluorescent images of Lucifer yellow gradient across the gap channel. Images taken at 5 min, 10min, 1.5 hour and 3 hour are shown here.

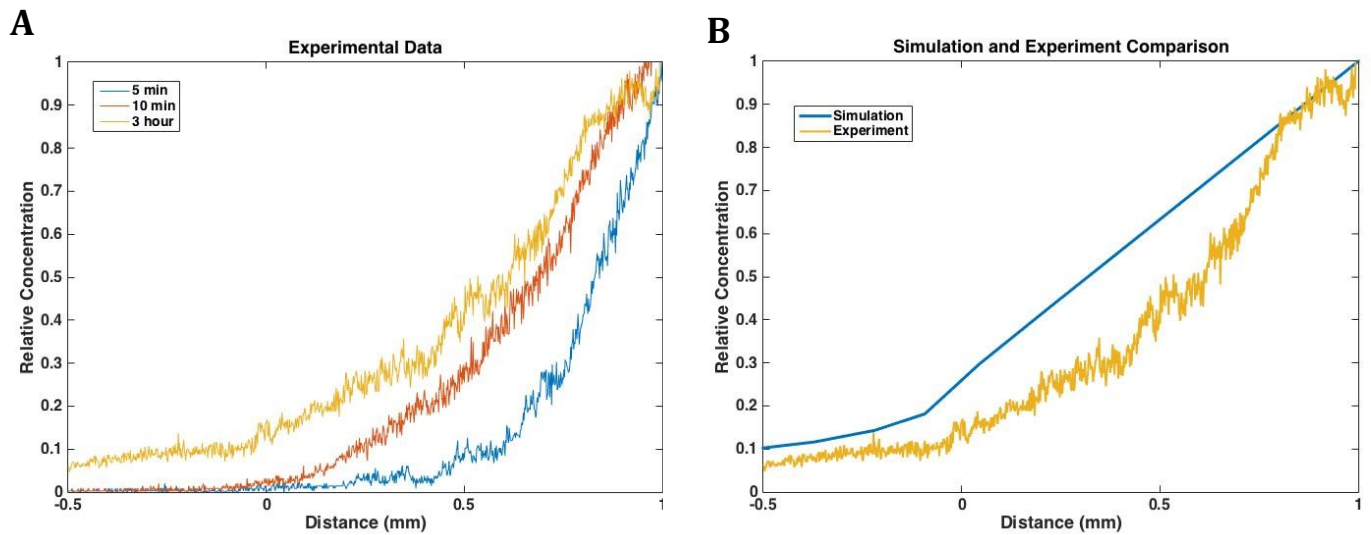


Figure 20. Concentration profiles generated based on the fluorescent intensity. **A)** Concentration profiles at 5 min, 10 min and 3 hours. **B)** Comparison between COMSOL simulation and experimental results.

4.3 HUVEC Cell Seeding

4.3.1 Evaluation

After seeding HUVEC cells in the EC channel, cell attachment and viability were observed using bright-field images and live/dead staining. Bright-field images were taken at 1.5 hours after seeding and day 1. Live and dead staining was performed on day 1 following the manufacturer's instructions. Both bright-field image and fluorescent images were taken using Olympus IX50 microscope.

4.3.2 Results

Several attempts have been made to seed HUVECs in the EC channel. Following the procedure reported in section 3.5, I provide results of one of the experiments. After 1.5 hours of inter-compartmental flow, cell attachment was observed on the bottom surface of the channel and at the gel interface (**Figure 21A**). We then switched to a circulating flow using the peristaltic pump. After one day of flow, cells attached to the bottom showed good morphology (**Figure 21B**), while most of the cells at the hydrogel interface had detached. Live and dead staining also showed good cell viability at the bottom of the channel (**Figure 22**). There are very few dead cells as the cells with low viability are likely to be washed away under the flow. The cause of the detachment at the collagen interface was still elusive. The most likely explanation is the stress resulted from the inter-compartmental flow. Since the flow powered by peristaltic pumps is pulsed, cells attached on collagen constantly experienced oscillating flow passing through the gap channel. The stress resulted from the flow could cause endothelial cell detachment.

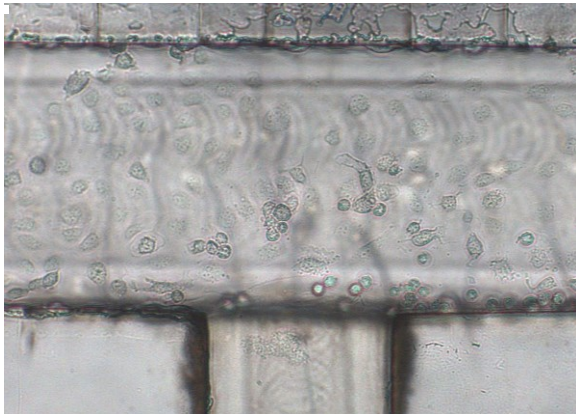
A



B



C



D

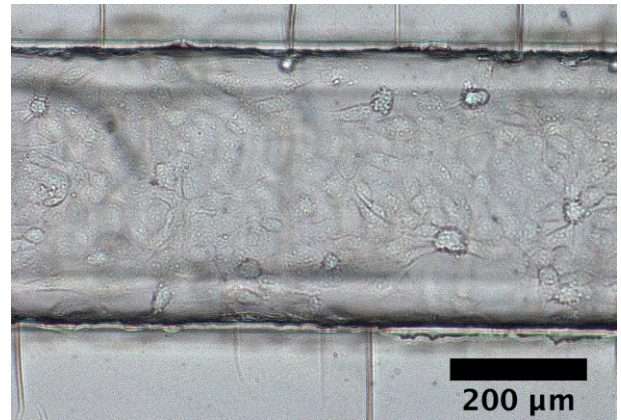
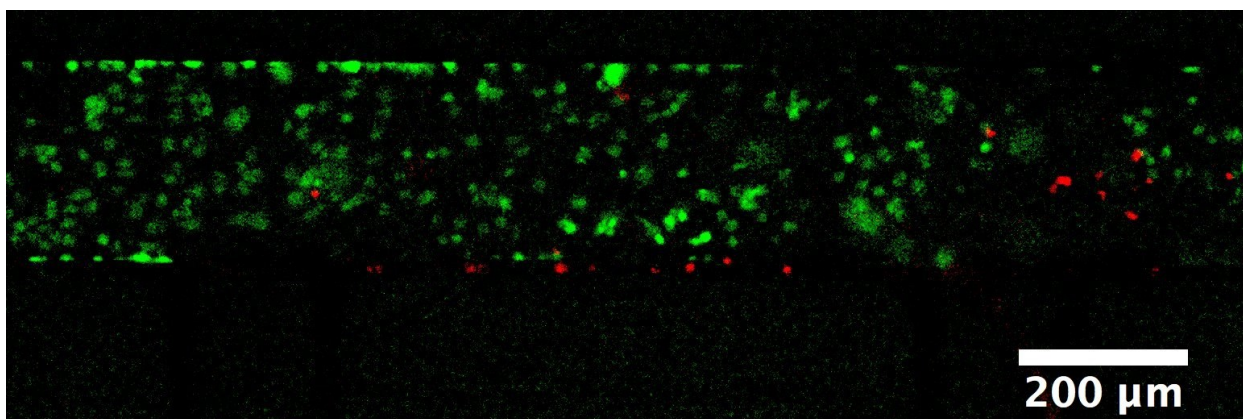
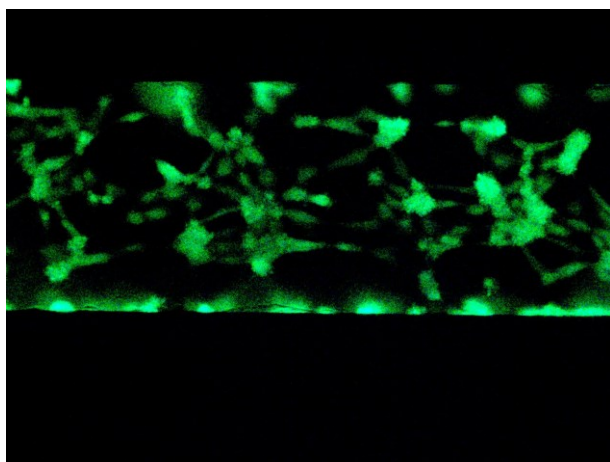


Figure 21. EC channel bright-field images. **A)** 4X bright-field image of the HUVEC cells after 1.5 hour inter-compartmental flow. **B)** 4X bright field image taken on day 1. **C)** 10X bright field image taken on day 1 at the gel interface. **D)** 10X bright-field image of the EC channel taken on day 1.

A



B



C

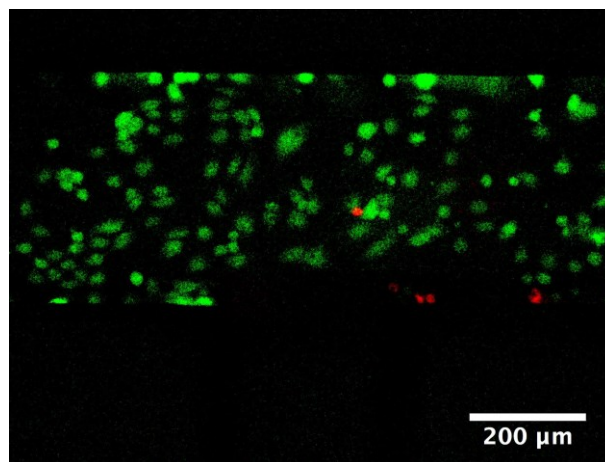


Figure 22. EC channel live and dead staining. **A)** 4X fluorescent image of the HUVEC cells on day 1. **B)** 10X fluorescent image of the EC channel. **C)** 10X fluorescent image taken at the gel interface

5. Discussion

5.1 Overview

In this project, we developed a microfluidic system that could be used to study the effects of concentrations and gradients of soluble molecules in the tumor microenvironment on cancer cell invasion and intravasation. As indicated by the oxygen reading and Lucifer yellow diffusion test, the device allows effective control of different chemical concentrations, such as dissolved oxygen, experienced by the cancer cells, while leaving the endothelial cells unaffected. Cell seeding experiments indicate that the design of the system could support cell survival. Generating a continuous endothelial monolayer was shown to be difficult and would be an important topic to explore in the future.

5.2 Flow System and Concentration Control

One of the primary challenges of the project was the design of the flow system (**Figure 4 & 5**). Using a peristaltic pump to drive the circulating flow is a simple design that also provides good control over the flow rate. The results of the oxygen reading showed that the design allowed independent control of different chemical concentrations, including dissolved gas in the two compartments (**Figure 17 & 18**). This enabled us to test how concentrations and gradients of different molecules in the cancer microenvironment could affect cancer cell behaviors while keeping the cell culture conditions in the EC channel throughout the experiments.

A limitation of the design was that the impulse flow generated by the peristaltic pump resulted in inter-compartment flow through the gap channel. While the inter-compartmental flow had little effects on the chemical concentrations in the two compartments, it would

likely alter the gradients along the gap channel. The Lucifer yellow diffusion test was performed using gravity driven flow, and the results demonstrate that we could generate a stable gradient in the absence of significant inter-compartmental flow (**Figure 19 & 20**). The exact effect of inter-compartmental flow on the gradient would need to be further tested, but it would certainly need to be minimized.

In addition, the inter-compartmental flow could have serious negative effects on the cells cultured in the device. As discussed in section 5.4.2, it is highly likely that the stress resulting from inter-compartmental flow caused the endothelial cell detachment at the hydrogel interface.

An alternative flow system design is gravity drive system. A gravity driven system generates smooth and stable flow, but still presents difficulties in balancing the pressure between the two compartments and preventing inter-compartmental flow. Besides, it is challenging to precisely control the flow rate using gravity driven flow. When assembling the gravity driven system for the Lucifer yellow gradient test, a significant amount of time was spent determining the correct reservoir placement to achieve pressure balance and generate the desired flow rate.

5.3 HUVEC Seeding

Developing the EC channel seeding protocol is an important part of the project. An early challenge was providing sufficient oxygen for the newly seeded cells without interfering with the initial attachment. Cell seeding in PDMS devices usually allows cells to attach statically for a couple hours, and the high oxygen permeability of PDMS allows cells to obtain oxygen diffused from the outer environment. Since our device was made out of oxygen impermeable

PMMA, oxygen would deplete quickly without media flow, and static attachment would not be feasible. To solve the problem, we created an inter-compartmental flow going from the EC channel to the cancer compartment. The flow not only provided the needed oxygen for cells, but also helped move cells onto the hydrogel interface to generate an endothelial monolayer. As shown in the figure 19, after 1.5 hours of inter-compartmental flow, there was a significant amount of cells attached. Compared to other trials that allowed a short duration for static attachment, inter-compartmental flow achieved the best cell attachment results. Another existing challenge was to maintain the continuous monolayer at the delicate and soft hydrogel interface. Many trials successfully generated an endothelial monolayer after inter-compartmental flow, but cells at the interface detached on day 1 after a period of peristaltic flow. The exact reason for cell detachment is still unclear, but we hypothesized that it resulted from the stress caused by inter-compartmental flow. Cell morphology and live dead staining indicated good cell viability at the bottom surface of the channel (**Figure 20 & 21**), excluding the possibility that cell detachment was caused by cytotoxicity, insufficient oxygen, or inadequate nutrition supply. To find the actual reason, time-lapse experiments could provide valuable information about how the detachment really happened. If, for example, the detachment was caused by inter-compartmental flow, modifying channel design and improving flow system would be important steps necessary for solving the problems.

5.4 Future Remarks

There were several limitations on this project due to time constraints. Our endothelial cell seeding protocol would need to be further investigated. Based on the experimental results achieved in this project, a flow system that could generate smoother flow might provide better results. Furthermore, the underlying biological problems that motivated the

development of this microfluidic system were not explored. The design of the device allows live-time observations, and cell migration could be studied using 3D tracking under a fluorescent microscope. However, fitting the entire system onto the scope would still be difficult. Currently, the device only has two gap channels that connect the cancer compartment with the EC channel, limiting the number of cell that migrate and interact with the endothelial cells. One solution is to add more gap channels to the device. Since passive diffusion is a slow process, additional gap channels will not damage independent concentration control in the two compartments, given that there is no significant inter-compartmental flow across the gap channels. Another solution is to connect multiple devices in parallel to increase the sample size obtainable in one experiment. Only after addressing these technical challenges could this device be useful for observing how altered concentrations and gradients in the tumor microenvironment can promote cancer metastasis.

Citation

1. Guan X. Cancer metastases: challenges and opportunities. *Acta Pharm Sin B*. 2015;5(5):402-18.
2. Li Z, Li Z. Glucose regulated protein 78: a critical link between tumor microenvironment and cancer hallmarks. *Biochim Biophys Acta*. 2012;1826(1):13-22.
3. Gilkes DM, Semenza GL, Wirtz D. Hypoxia and the extracellular matrix: drivers of tumour metastasis. *Nat Rev Cancer*. 2014;14(6):430-9.
4. Rankin EB, Giaccia AJ. Hypoxic control of metastasis. *Science*. 2016;352(6282):175-80.
5. Sahlgren C, Gustafsson MV, Jin S, Poellinger L, Lendahl U. Notch signaling mediates hypoxia-induced tumor cell migration and invasion. *Proceedings of the National Academy of Sciences of the United States of America*. 2008;105(17):6392-7.
6. Hirayama A, Kami K, Sugimoto M, Sugawara M, Toki N, Onozuka H, et al. Quantitative metabolome profiling of colon and stomach cancer microenvironment by capillary electrophoresis time-of-flight mass spectrometry. *Cancer research*. 2009;69(11):4918-25.
7. Funamoto K, Zervantonakis IK, Liu Y, Ochs CJ, Kim C, Kamm RD. A novel microfluidic platform for high-resolution imaging of a three-dimensional cell culture under a controlled hypoxic environment. *Lab Chip*. 2012;12(22):4855-63.
8. Cheema U, Rong Z, Kirresh O, MacRobert AJ, Vadgama P, Brown RA. Oxygen diffusion through collagen scaffolds at defined densities: implications for cell survival in tissue models. *J Tissue Eng Regen Med*. 2012;6(1):77-84.
9. Rong Z, Cheema U, Vadgama P. Needle enzyme electrode based glucose diffusive transport measurement in a collagen gel and validation of a simulation model. *Analyst*. 2006;131(7):816-21.
10. Abaci HE, Devendra R, Smith Q, Gerecht S, Drazer G. Design and development of microbioreactors for long-term cell culture in controlled oxygen microenvironments. *Biomed Microdevices*. 2012;14(1):145-52.
11. Abaci HE, Devendra R, Soman R, Drazer G, Gerecht S. Microbioreactors to manipulate oxygen tension and shear stress in the microenvironment of vascular stem and progenitor cells. *Biotechnol Appl Biochem*. 2012;59(2):97-105.
12. Herst PM, Berridge MV. Cell surface oxygen consumption: a major contributor to cellular oxygen consumption in glycolytic cancer cell lines. *Biochim Biophys Acta*. 2007;1767(2):170-7.
13. Wagner BA, Venkataraman S, Buettner GR. The rate of oxygen utilization by cells. *Free Radic Biol Med*. 2011;51(3):700-12.
14. Cochran DM, Fukumura D, Ancukiewicz M, Carmeliet P, Jain RK. Evolution of oxygen and glucose concentration profiles in a tissue-mimetic culture system of embryonic stem cells. *Ann Biomed Eng*. 2006;34(8):1247-58.
15. Gong X, Yi X, Xiao K, Li S, Kodzius R, Qin J, et al. Wax-bonding 3D microfluidic chips. *Lab Chip*. 2010;10(19):2622-7.
16. Rafat M, Raad DR, Rowat AC, Auguste DT. Fabrication of reversibly adhesive fluidic devices using magnetism. *Lab Chip*. 2009;9(20):3016-9.

17. Anwar K, Han T, Kim SM. Reversible sealing techniques for microdevice applications. *Sensors and Actuators B: Chemical*. 2011;153(2):301-11.
18. Chen Z, Gao Y, Lin J, Su R, Xie Y. Vacuum-assisted thermal bonding of plastic capillary electrophoresis microchip imprinted with stainless steel template. *Journal of Chromatography A*. 2004;1038(1-2):239-45.
19. Nguyen-Ngoc KV, Ewald AJ. Mammary ductal elongation and myoepithelial migration are regulated by the composition of the extracellular matrix. *J Microsc*. 2013;251(3):212-23.

Yu Xu

Phone: 646-204-2350
Email: yxu33@jhu.edu

Education:

Johns Hopkins University
MSE Candidate, Biomedical Engineering

Baltimore, MD
Expected July 2017

Johns Hopkins University
BS, Biomedical Engineering
Minor in Applied Mathematics and Statistics
-Overall GPA: 3.93

Baltimore, MD
May 2016

Research Experience:

Institute for NanoBioTechnology, Johns Hopkins University
Researcher, Gerecht Lab

Baltimore, MD
Fall 2013 - Present

- Currently developing a microfluidic device to study the effects of hypoxia and glucose deprivation on cancer intravasation.
- **Past Project 1:** Used a novel oxygen controllable hydrogel to test the effects of hypoxic gradient on sarcoma cell invasion.
- **Past Project 2:** Used a microfluidic device to study the effects of hypoxia and TNF-alpha stimulation on endothelial progenitor cell recruitment during wound healing.

Cutaneous Biology Research Center, Massachusetts General Hospital
Research Assistant, Fisher Lab

Boston, MA
Summer 2015

- Studied combination immunotherapy for melanoma

Huashan Hospital, Fudan University
Research Assistant

Shanghai, China
Summer 2013

- Studied the synergistic effect of icaritin and vemurafenib on melanoma.

Teaching Experience:

Johns Hopkins University
Teaching Assistant, Systems Bioengineering Lab

Baltimore, MD
Fall 2016 – Spring 2017

- Assisted students to finish lab assignments, held office hours to help students with questions, and graded homework and exams.

Publications:

Intratumoral oxygen gradients mediate sarcoma cell invasion

D Lewis, K Park, V Tang, **Yu Xu**, K Pak, T Eisinger-Mathason, M Simon, S Gerecht; Proc Natl Acad Sci U S A. 2016; 113(33): 9292-7.

Melanoma Immunotherapy: mechanisms and opportunities

Yu Xu, A Van Der Sande, J Lo, D Fisher; Invest Dermatol Venereol Res. 2015; 2(1): 1-7.

Endothelial progenitor cell recruitment in a microfluidic vascular model

D Lewis, H. Abaci, **Yu Xu**, S Gerecht; Biofabrication. 2015; 7(4)

Patents:

Orthosis to Mitigate Cerebral Palsy Scissoring Gait

(Pending) PCT/US2016/030883

Filed on May 05, 2016 with Johns Hopkins Tech Transfer Office

Spill-Proof Cup for People with Cerebral Palsy

(Pending) PCT/US2016/034941

Filed on May 31, 2016 with Johns Hopkins Tech Transfer Office

Honors and Awards:

Richard J. Johns Award

May 2016

- Awarded to students who have achieved a high level of academic accomplishment in their undergraduate years.

Student Initiatives Fund

April 2015

- Given by Johns Hopkins School of Engineering to support self-motivated engineering projects
- Project to develop an orthosis to mitigate the symptoms of scissor gait for people with cerebral palsy.

World Cerebral Palsy Day Prize

July 2014

- International competition that aims to gather ideas and inventions to improve the lives of people with cerebral palsy (CP).
- Project to develop a spill-proof cup to accommodate drinking difficulties faced by people with CP.

Provost's Undergraduate Research Award

May 2014

- Given by the Johns Hopkins University to support undergraduate research projects
- Project to reconstruct an ancient Chinese rocket.

Extracurricular Activities:

Tutorial Project, Johns Hopkins University

Baltimore, MD

Tutor

Spring 2013, Spring 2015 – Spring 2016

- Provided one-on-one tutoring for elementary school students in math and reading

Advocates for Autism, Johns Hopkins University

Baltimore, MD

Student Volunteer

Fall 2013 – Spring 2016

- Raised the awareness of autism by organizing events such as inviting speakers to give lectures.
- Volunteered at the Kennedy Krieger Institute and interacted with children in the playground

Musicare, Johns Hopkins University

Baltimore, MD

Student Volunteer

Fall 2013 – Present

- Perform piano for patients in hospitals

Society for Biomaterials, Johns Hopkins University

Baltimore, MD

Member and Webmaster,

Fall 2013 – Present

- Organize events, such as inviting guest speakers, to promote student interest in biomaterials
- Created and maintain group website

Skills:

Laboratory Techniques: Mammalian cell culture, Microfluidics fabrication, Immunofluorescent staining, Florescence microscopy, Western blot, RT-PCR, ELISA.

Software: Creo Parametric, Autodesk Inventor, MATLAB, ImageJ, GraphPad Prism, IMARIS, Adobe Illustrator, Adobe Premiere

Language: Native Chinese Speaker